Debris disks as seen by Herschel[*]/DUNES

T. Löhne[1,**], **C. Eiroa**[2], **J.-C. Augereau**[3], **S. Ertel**[4], **J.P. Marshall**[2], **A. Mora**[5], **O. Absil**[6], **K. Stapelfeldt**[8], **P. Thébault**[9], **A. Bayo**[10], **C. del Burgo**[11], **W. Danchi**[15], **A.V. Krivov**[1], **J. Lebreton**[3], **G. Letawe**[6], **P. Magain**[6], **J. Maldonado**[2], **B. Montesinos**[7], **G.L. Pilbratt**[12], **G.J. White**[13], and **S. Wolf**[4]

[1] Astrophysikalisches Institut und Universitätssternwarte, Friedrich-Schiller-Universität Jena, Schillergäßchen 2–3, 07745 Jena, Germany

[2] Departmento Física Teórica, Facultad de Ciencias, Universidad Autónoma de Madrid, Cantoblanco, 28049 Madrid, Spain

[3] UJF-Grenoble 1 / CNRS-INSU, Institut de Planétologie et d'Astrophysique de Grenoble (IPAG) UMR 5274, 38041 Grenoble, France

[4] Christian-Albrechts-Universität zu Kiel, Institut für Theoretische Physik und Astrophysik, Leibnizstr. 15, 24098 Kiel, Germany

[5] ESA-ESAC Gaia SOC. PO Box 78 28691 Villanueva de la Cañada, Madrid, Spain

[6] Institut d'Astrophysique et de Géophysique, Université de Liège, allée du 6 août 17, 4000 Liège, Belgium

[7] Departmento de Astrofísica, Centro de Astrobiología (CAB, CSIC-INTA), ESAC Campus, PO Box 78, 28691 Villanueva de la Cañada, Madrid, Spain

[8] Jet Propulsion Laboratory, California Institute of Technology, Pasadena, CA 91109, USA

[9] LESIA, Observatoire de Paris, 92195 Meudon Principal Cedex, France

[10] European Southern Observatory, Alonso de Córdova 3107, Vitacura, Santiago, Chile

[11] UNINOVA-CA3, Campus da Caparica, Quinta da Torre, Monte de Caparica, 2825-149 Caparica, Portugal

[12] ESA Astrophysics & Fundamental Physics Missions Division, ESTEC/SRE-SA, Keplerlaan 1, 2201 AZ Noordwijk, The Netherlands

[13] Department of Physics and Astrophysics, Open University, Walton Hall, Milton Keynes MK7 6AA, UK

[14] Rutherford Appleton Laboratory, Chilton OX11 0QX, UK

[15] NASA Goddard Space Flight Center, Exoplanets and Stellar Astrophysics, Code 667, Greenbelt, MD 20771, USA

The far-infrared excesses produced by debris disks are common features of stellar systems. These disks are thought to contain solids ranging from micron-sized dust to planetesimals. Naturally, their formation and evolution are linked to those of potential planets. With this motivation, the Herschel open time key programme DUNES (DUst around NEarby Stars) aims at further characterising known debris disks and discovering new ones in the regime explored by the Herschel space observatory. On the one hand, in their survey of 133 nearby FGK stars, DUNES discovered a class of extremely cold and faint debris disks, different from well-known disks such as the one around Vega in that their inferred typical grain sizes are rather large, indicating low dynamical excitation and low collision rates. On the other hand, for the more massive disk around the sun-like star HD 207129, well-resolved PACS images confirmed the ring-liked structure seen in HST images and provided valuable information for an in-depth study and benchmark for models. Employing both models for power-law fitting and collisional evolution we found the disk around HD 207129 to feature low collision rates and large grains, as well. Transport by means of Poynting-Robertson drag likely plays a role in replenishing the dust seen closer to the star, inside of the ring. The inner edge is therefore rather smooth and the contribution from the extended halo of barely bound grains is small. Both slowly self-stirring and planetary perturbations could potentially have formed and shaped this disk.

1 Introduction

Since 1983, several hundred debris disks have been discovered by various infrared facilities, e.g., IRAS, ISO, JCMT/SCUBA, Spitzer, AKARI, and now Herschel and WISE, because it is the excess thermal emission of these disks' dust components that is most easily detectable. Their observations have revealed a wide variety of inferred dust masses, disk extents, and even disk morphologies (e.g., Wyatt 2008, and references therein). Dust has been detected from well within one AU (Absil et al. 2006; Beichman et al. 2005), out to hundreds of AU (e.g., Su et al. 2005). The latter are more commonly reported, corresponding to significantly higher detection rates at longer wavelengths. In

---

addition, with regard to current sensitivity limits, a population of disks that are cold but rich in dust could still be hidden. Some of these are revealed by Herschel (Eiroa et al. 2011; Pilbratt et al. 2010).

2 The DUNES programme

DUNES (DUst around NEarby Stars) is a Herschel open-time key programme designed to detect and characterise cold and faint debris disks, sized-up analogues to the Kuiper belt, around a statistically meaningful sample of nearby main-sequence FGK stars, taking advantage of the unique combination of wavelength coverage, sensitivity, and resolution of Herschel with PACS (Poglitsch et al. 2010) and SPIRE (Griffin et al. 2010). The data is analysed with a set of radiative, collisional and dynamical dust disk models.

2.1 Strategy and sample

The DUNES objectives require the detection of very faint excesses at the mJy level, comparable to the photospheric emission and only a few times the measurement uncertainties. The primary observing strategy is designed to integrate for as long as needed to detect the 100 μm photospheric flux at a 5- to 7-σ level, subject only to confusion noise limitations. These data are accompanied by images in the red channel (160 μm). The maximum distance was set to 21 pc, fitted to the total observing time of 140 hours granted by the Herschel time allocation committee. The survey is therefore only volume-limited and unbiased with respect to distance and spectral class. We complemented the sample with the remaining systems with known planets (as of 2008) within 25 pc from the Sun owing to their special scientific interest. Under these constraints, a total of 133 main-sequence FGK stars were selected and successfully observed by summer 2011. Where promising, additional images were acquired with PACS (at 70/160 μm) and SPIRE (at 250, 350, and 500 μm).

First results have been published in Eiroa et al. (2010) and a detailed description of the observing strategy and the sample characteristics will be presented in a forthcoming paper (Eiroa et al., in prep.).

2.2 Cold disks

Herschel's sensitivity and wavelength range define the regime where new discoveries were to be expected: that of cold and faint disks. These expectations were fulfilled by DUNES. Based on Herschel/PACS images and photometry, Eiroa et al. (2011) report on the discovery of a new class of disks with significant excess emission at 160 μm, no or little excess at 100 μm, and no excess at shorter wavelengths. The typical temperature of this excess is $\lesssim 22$ K. This temperature is remarkably low compared to the blackbody estimates (or lower limits) based on the resolved physical extents (or upper limits thereof). It can only be explained by

a low absorption efficiency of starlight in the optical and a high emission efficiency in the far infrared. The latter also requires the grains to be large compared to the radiation pressure blowout limit – in contrast to the smaller grains expected in a collisionally active debris disk. The observed emission properties might therefore hint to a dynamically cold state, where small grains are depleted (see, e.g., Thébault & Wu 2008; Vitense et al. 2010). On the other hand, large, kilometre-sized planetesimals might also be absent because of too long a timescale for growth. In summary, these disks eventually exist somewhere in between crowded planetary systems in full bloom and the vast nothingness (no offence) of interstellar space.

3 HD 207129

Most of the known debris disks have been characterised using spectral and photometric data, with only a few dozen having been spatially resolved. When it comes to modelling, these sparse data sets unavoidably introduce degeneracies between the properties of grains (particularly their typical sizes and distances to the star). A given observed colour temperature could, for example, correspond to larger grains closer to the star or smaller ones further away. The success in finding trends and characterising a typical debris disk depends crucially on the few objects where these degeneracies have been broken. Good knowledge of a set of such archetypes eases the navigation in parameter space and allows for the calibration of simpler models.

In this section, we discuss the modelling of the HD 207129 system. The host star is of nearly sun-like spectral type and luminosity with an estimated age of 1.5–3.2 Gyr (Marshall et al. 2011, and references therein). Excess emission was first detected by IRAS (Walker & Wolstencroft 1988), and later observed by ISO (Jourdain de Muizon et al. 1999), Spitzer (Trilling et al. 2008), and APEX (Nilsson et al. 2010). The scattered light images obtained with the Hubble Space Telescope (HST) (Krist et al. 2010) have shown a prominent inclined ring at a distance of 163 AU to the star – the most distant known source region for debris dust.

The best images so far have been obtained with Herschel/PACS and SPIRE in the framework of the DUNES survey (Marshall et al. 2011). Again, a ring-like outer disk is visible, separated from the star by an inner depletion zone. This inner hole, the sheer size of the disk, and the data quality render HD 207129 an interesting object to study.

This study is presented in full extent in Löhne et al. (2012).

3.1 Observations

Our modelling is centred on the observational results presented in Marshall et al. (2011). These data were obtained with Herschel/PACS and SPIRE in scan map and small map modes, respectively. With the photometry from both
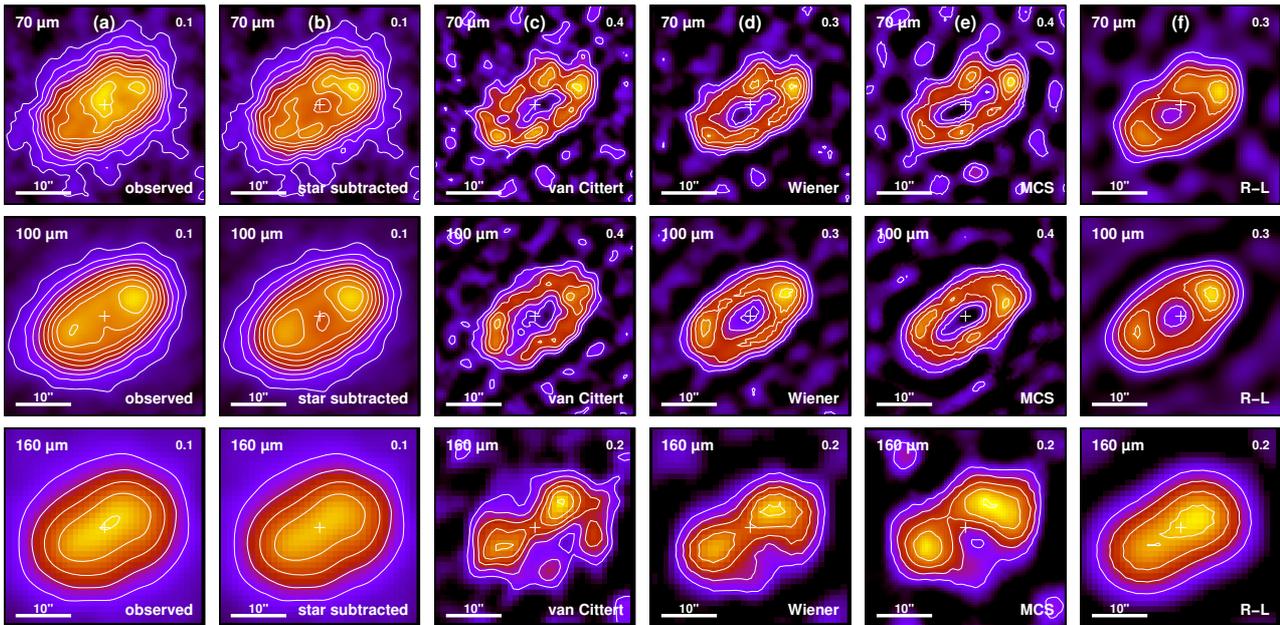
Fig. 1   Herschel/PACS images of HD 207129 at (*top to bottom*) 70, 100, and 160 μm. Columns (a) and (b) show the observed and star-subtracted images, respectively. Columns (c) to (f) show deconvolved images using the following methods: (c) van Cittert, (d) FFT with a Wiener filter, (e) MCS code, (f) Richardson–Lucy. Flux steps (in mJy/arcsec^2) between solid isolines are indicated in the top-right corner of each panel. The photocentre of the disk, i.e. the assumed stellar position, is indicated by a cross. In every panel, North is up and East is left.

instruments, the SED is more densely sampled, and PACS images (see Fig. 1) additionally yield spatially resolved brightness information. Photospheric estimates for modelling and star subtraction are based on PHOENIX/NextGen models (Hauschildt et al. 1999), normalised to the short-wavelength, non-excess part of the Spitzer/IRS spectrum.

3.2   Power-law modelling

For a first estimate of the properties of the dust, we started with an empirical fitting of its size and radial distributions. For this fitting we used both a scheme based on simulated thermal annealing (Press et al. 1992, SAnD; see S. Ertel et al., submitted to A&A) and a Bayesian approach with extensive χ^2 mapping of the parameter space (GRaTer; see Augereau et al. (1999) and J.-Ch. Augereau et al., in prep., on models of the q^1 Eridani debris disk).

The distribution of surface number density n, i.e. the number of particles per unit size and (normal) disk area, was parameterised with two separate power laws for size and radial distributions

$$n(s,r) = n_0 \left(\frac{s}{s_0}\right)^\kappa \left(\frac{r}{r_0}\right)^\alpha \propto s^\kappa r^\alpha, \qquad (1)$$

where we assumed grain sizes $s \in [s_{\min}, s_{\max}]$ and the distances $r \in [r_{\min}, r_{\max}]$ with $s_0 = s_{\min}$ and $r_0 = r_{\max}$. The boundaries and the exponents were free parameters.

The best-fit setup includes dust with a weekly constrained ice content $\sigma_{\text{ice}} = 50\%$ and a surface density rising from $r_{\min} \lesssim 60$ AU towards an outer edge at or slightly
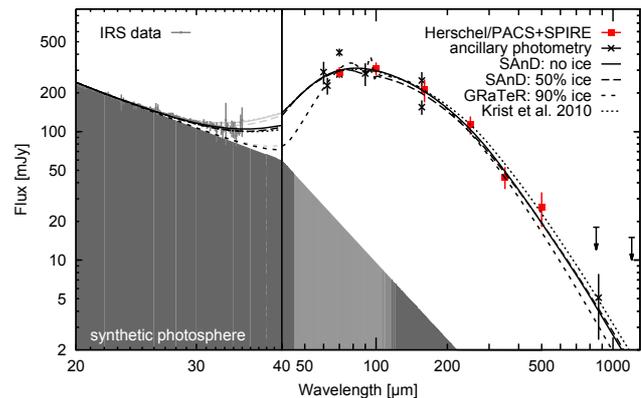
Fig. 2   Spectral energy distributions of the best-fit power law-based models. The photometry points used for the fitting are overplotted. Note that the horizontal stretch is different for wavelengths smaller than 40 μm. To compare the models to the IRS data from the standard pipeline, we corrected the model SEDs for slit loss and then applied a point-source correction. The uncorrected model SEDs are plotted with light grey lines.

beyond the outer edge of the HST ring (178 AU). The radial slope is $\alpha = 2 \ldots 3.5$. Although the inner edge is also weekly constrained, the results (see Fig. 2 and top panels of Fig. 3) show that a narrow outer ring alone (as inferred from the HST observations) cannot reproduce the observed radial profiles and that additional material is present inside of the ring.

Such a radial profile that rises outward with a sharp *outer* edge contrasts with those derived for the archetypal
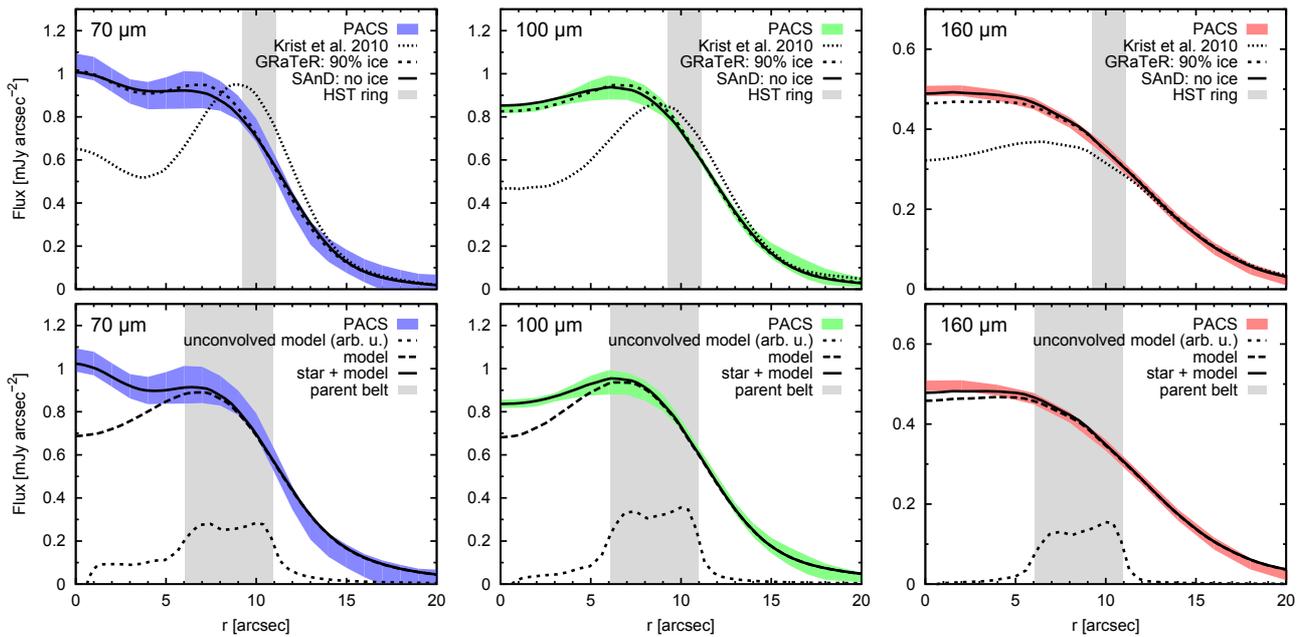
Fig. 3 Radial brightness profiles along the long disk axis at (*left*) 70 μm, (*middle*) 100 μm, (*right*) 160 μm. *Top*: best-fit power-law results obtained with GRaTer and SAnD compared to the model of Krist et al. (2010). *Bottom*: reference run of the collisional model with and without stellar contribution.

disks Vega (Krivov et al. 2006; Müller et al. 2010; Sibthorpe et al. 2010; Su et al. 2005) and β Pictoris (Golimowski et al. 2006; Krivov et al. 2009; Thébault & Wu 2008; Vandenbussche et al. 2010). In these disks, the derived geometrical optical thickness typically falls off with a moderate $r^{-1.5}$ relationship beyond the peak value, i.e. they do not feature sharp outer edges. Disks are instead often assumed to have *inner* edges as sharp as that of Fomalhaut (Kalas et al. 2008, 2005), for example.

3.3 Collisional modelling

We now seek to more tightly constrain the properties of the dust disk by modelling the production and loss of material in the collisional cascade that is assumed to act in a debris disk. In this approach, the distributions of sizes and radial distances of the dust are coupled and can no longer be directly controlled. Instead, they are replaced as free parameters by the (initial) parameters of the underlying planetesimal disk.

The approach is translated into a kinetic problem, where collision rates and outcomes are described statistically. The numerical solution to this problem is implemented in a parallel C++ code (ACE, Analysis of Collisional Evolution). A more detailed description of the model can be found in earlier papers (Krivov et al. 2005, 2006, 2008).
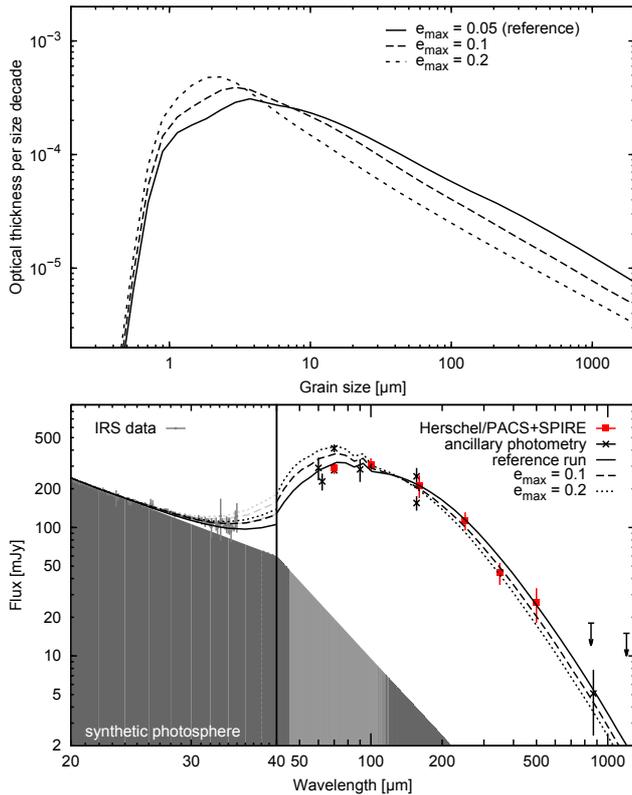
In agreement with the results of Sect. 3.2, we find a reference setup where most material is concentrated near the outer disk edge. The initial slope of the radial profile of optical depth (or surface mass density) is $\alpha = 3.5$, i.e. rising steeply outwards. The maximum orbital eccentricity of the
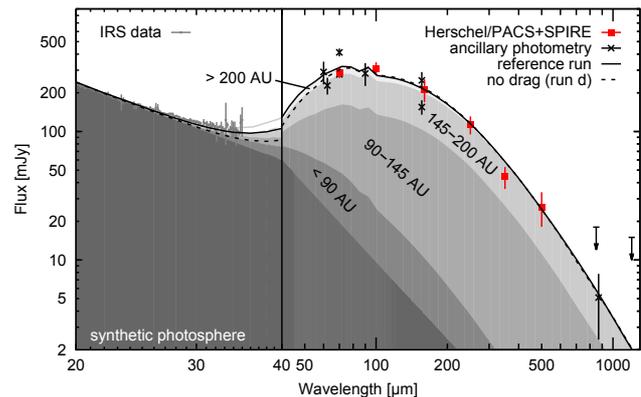
Fig. 4 Same as Fig. 2 but for the spectral energy distribution of the reference run and the contributions from its constituent annuli and the star. For comparison, a run without Poynting-Robertson drag (run d) is dashed.

larger grains and the parent bodies is $e_{max} = 0.05$, corresponding to a low dynamical excitation, i.e. low collisional velocities. At 4–8 μm, the radii of the grains that dominate the cross-section are by about a factor of ten above the blowout limit – considerably larger than what is predicted for collisionally active disks (Krivov et al. 2006; Thébault et al. 2003).
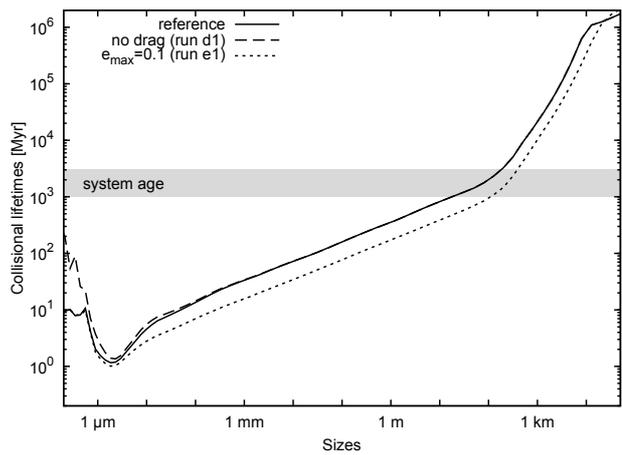
The radial profiles in the bottom panels of Fig. 3 and the SED in Fig. 4 illustrate that this reference run agrees with the observations to a degree that is comparable with the power-law fits. As in Sect. 3.2, the absolute flux at 100 μm is underpredicted by about 18 % (see SED).

Fig. 6 (online colour at: www.an-journal.org) Collisional and transport lifetimes of objects in (black solid line) the reference run, (dashed line) the dragless run d, and (dotted line) run e1.

for grains smaller than 1 mm. For grains smaller than about 1 μm, transport even becomes the dominant loss channel, acting on timescales much shorter than the purely collisional timescales. For these grains, an increase in the mass throughput of the collisional cascade, as in run e1, has no effect.

3.4 Discussion

Both power-law fitting and collisional modelling indicate that most of the material is concentrated near the outer edge of the underlying distribution of unseen parent bodies – where the inclined ring has been observed at around 163 AU with the HST (Krist et al. 2010). The HD 207129 disk then features a rather sharp outer edge while other debris disks are often surrounded by haloes of small grains. Significant amounts of dust are found to be present within the inner edge of the ring, though with a profile that steeply rises outward. The inner cutoff of the dust distribution is likely located within 60 AU from the central star. A massive planet that shepherds the inner edge of the ring (as Fomalhaut b potentially does) is probably absent.

From the low temperatures and the accordingly large effective grain sizes, we can conclude that the dynamical excitation of the disk is low and transport by P–R drag plays a notable role. We deduce that the rate of collisions is lower in accordance with the typical eccentricities $e_{max} \leq 0.05$. While being dominated by collisions, large grains also get dragged inward and notably fill the inner gap in surface brightness, the more so at shorter wavelengths.

In our modelling we were able to put only weak constraints on the chemical composition. We verified that it is possible to produce good fits with both high silicate fractions and high ice fractions. The greatest differences occur at short wavelengths, where the Spitzer/IRS data are most consistent with moderate mixing ratios.

With its low dynamical excitation and its brightness peaking at an unprecedented radial distance of about

Fig. 5 (online colour at: www.an-journal.org) *Top*: size distribution in terms of optical depth at 150 AU as a function of grain size. The reference run is compared with runs e1 (where $e_{max} = 0.1$) and e2 (where $e_{max} = 0.2$). *Bottom*: spectral energy distribution of the reference and runs e1 and e2.

Figure 5 shows that a higher dynamical excitation notably increases the typical temperature by reducing the typical grain size. The reason is that the dynamical excitation determines the ratio of the number of large grains, which inherit the excitation of the parent bodies, to the number of small grains that are affected by radiation pressure (Thébault & Wu 2008). By considering both the SED and the radial profiles, we can constrain the dynamical excitation of the disk to values of $e_{max} \leq 0.05$, i.e. $\langle e \rangle \leq 0.025$ and $\langle i \rangle \leq 0.0125 = 0.75°$ (assuming that e and i are distributed uniformly). The excitation is lower than what is typically expected for efficient stirring by a planet (see, e.g. Gomes 2003; Wyatt 2003), lower than what is inferred from a similar model of the Vega disk (Müller et al. 2010, where $e_{max} = 0.2$) and lower than the average values for the classical, dynamically cold population of the Edgeworth–Kuiper belt: eccentricities $\langle e \rangle \approx 0.08$ and inclinations $\langle i \rangle \approx 2.7°$ (Brown 2001; Elliot et al. 2005; Vitense et al. 2010).

Figure 6 shows that the (collisional) lifetimes in the model disks are rather long. For objects larger than about 100 m the lifetimes are in fact longer than the estimated system age of 2 Gyr. These objects might still be primordial, i.e. not currently distributed as in collisional equilibrium. The comparison with the lifetimes for the dragless run additionally reveals that transport becomes noticeable

160 AU, HD 207129 might represent the limit to the population of coldest and most extended circumstellar debris disks detectable with Herschel.

4 Summary and outlook

The Herschel/DUNES programme delivered valuable new far-infrared photometry and images for already known debris disks and widened the detection space with the discovery of a new class of faint and cold disks. Both well-known individual objects and statistical data are vital to strengthen the theoretical understanding of the formation and evolution of debris disks. In-depth studies of a set of prominent, bright systems such as HD 207129 are needed to break the degeneracy between, e.g., grain size and disk radius – and thus to reduce the number of free parameters and calibrate simpler models for more general, statistical studies. In particular, the large grains around HD 207129 and the low dust temperatures in the "cold disks" indicate potential trends of increasing grain size with increasing disk radius or with reduced disk luminosity. It is however to early for more stringent or general conclusions. Nevertheless, these results on "unusual" debris disk will help define what a "usual" debris disk is.

References

Absil, O., di Folco, E., Mérand, A., et al.: 2006, A&A 452, 237

Augereau, J.-C., Lagrange, A.M., Mouillet, D., Papaloizou, J.C.B., Grorod, P.A.: 1999, A&A 348, 557

Beichman, C.A., Bryden, G., Rieke, G.H., et al.: 2005, ApJ 622, 1160

Brown, M.E.: 2001, AJ 121, 2804

Eiroa, C., Fedele, D., Maldonado, J., et al.: 2010, A&A 518, L131

Eiroa, C., Marshall, J.P., Mora, A., et al.: 2011, A&A 536, L4

Elliot, J.L., Kern, S.D., Clancy, K.B., et al.: 2005, AJ 129, 1117

Golimowski, D.A., Ardila, D.R., Krist, J.E., et al.: 2006, AJ 131, 3109

Gomes, R.S.: 2003, Icarus 161, 404

Griffin, M.J., Abergel, A., Abreu, A., et al.: 2010, A&A 518, L3

Hauschildt, P.H., Allard, F., Baron, E.: 1999, ApJ 512, 377

Jourdain de Muizon, M., Laureijs, R.J., Dominik, C., et al.: 1999, A&A 350, 875

Kalas, P., Graham, J.R., Chiang, E., et al.: 2008, Sci 322, 1345

Kalas, P., Graham, J.R., Clampin, M.: 2005, Nature 435, 1067

Krist, J.E., Stapelfeldt, K.R., Bryden, G., et al.: 2010, AJ 140, 1051

Krivov, A.V., Sremčević, M., Spahn, F.: 2005, Icarus 174, 105

Krivov, A.V., Löhne, T., Sremčević, M.: 2006, A&A 455, 509

Krivov, A.V., Müller, S., Löhne, T., Mutschke, H.: 2008, ApJ 687, 608

Krivov, A.V., Herrmann, F., Brandeker, A., Thébault, P.: 2009, A&A 507, 1503

Löhne, T., et al.: A&A 537, A110

Marshall, J.P., Löhne, T., Montesinos, B., et al.: 2011, A&A 529, A117

Müller, S., Löhne, T., Krivov, A.V.: 2010, ApJ 708, 1728

Nilsson, R., Liseau, R., Brandeker, A., et al.: 2010, A&A 518, A40

Pilbratt, G.L., Riedinger, J.R., Passvogel, T., et al.: 2010, A&A 518, L1

Poglitsch, A., Waelkens, C., Geis, N., et al.: 2010, A&A 518, L2

Press, W.H., Teukolsky, S.A., Vetterling, W.T., Flannery, B.P.: 1992, *Numerical recipes in FORTRAN. The art of scientific computing*, 2nd ed., Cambridge University Press, Cambridge

Sibthorpe, B., Vandenbussche, B., Greaves, J.S., et al.: 2010, A&A 518, L130

Su, K.Y.L., Rieke, G.H., Misselt, K.A., et al.: 2005, ApJ 628, 487

Thébault, P., Wu, Y.: 2008, A&A 481, 713

Thébault, P., Augereau, J.-C., Beust, H.: 2003, A&A 408, 775

Trilling, D.E., Bryden, G., Beichman, C.A., et al.: 2008, ApJ 674, 1086

Vandenbussche, B., Sibthorpe, B., Acke, B., et al.: 2010, A&A 518, L133

Vitense, C., Krivov, A.V., Löhne, T.: 2010, A&A 520, A32

Walker, H.J., Wolstencroft, R.D.: 1988, PASP 100, 1509

Wyatt, M.C.: 2003, ApJ 598, 1321

Wyatt, M.C.: 2008, ARA&A 46, 339